Local non–Calderbank-Shor-Steane quantum error-correcting code on a three-dimensional lattice

Isaac H. Kim

Phys. Rev. A **83**, 052308 — Published 12 May 2011

DOI: 10.1103/PhysRevA.83.052308

Local non-CSS quantum error correcting code on a 3D lattice

Isaac H. Kim
Institute of Quantum Information, California Institute of Technology, Pasadena CA 91125, USA

We present a family of non-CSS quantum error correcting code consisting of geometrically local stabilizer generators on a 3D lattice. We study the hamiltonian constructed from ferromagnetic interaction of overcomplete set of local stabilizer generators. The degenerate ground state of the system is characterized by a quantum error correcting code whose number of encoded qubits are equal to the second Betti number of the manifold. These models 1) have solely local interactions, 2) admit a strong-weak duality relation with an Ising model on a dual lattice 3) have topological order in the ground state, some of which survive at finite temperature, 4) behave as classical memory at finite temperature.

I. INTRODUCTION

One of the motivations for studying quantum error correcting code on lattice is to protect quantum information without active correction. Many models on 2D lattices have been proposed and analyzed [1–7] but no-go theorem rules out all finite-range finite-strength hamiltonian system in 2D as a self-correcting quantum memory.[8, 9] This does not apply to higher dimensions. For instance, it was shown that 4D toric code is a self-correcting quantum memory.[10, 11] Bombin et al. showed that there is also a 6D model that exhibits similar behavior.[12] Whether such thermally protected model exists in 3D remains as an open problem. 3D toric code can store classical information at finite temperature but it fails to do so for quantum information.[13] Toplogical color code in 3D, albeit lacking a rigorous proof, is believed to show a similar behavior: there exists a string-like logical operator which is thermally unstable.[14] 3D model proposed by Nussinov and Ortiz shows similar behavior.[15, 16] Another model was proposed by Chamon and analyzed recently by Bravyi et al. This model may be able to protect quantum information, but not in a thermodynamic sense.[17, 18]

It is worth noting that all the listed 3D models except Chamon's model share a similar property: the quantum error correcting code defining the ground state of the system is a Calderbank-Shor-Steane(CSS) code[19, 20], meaning that it can be decomposed into two classical codes. CSS code is a special kind of quantum error correcting code that can be described by stabilizer formalism.[21] These quantum error correcting codes can be 'stabilized' by a set of stabilizer group generators, meaning they are simultaneous $+1$ eigenstate of the group elements. If there exists a set of generators which can be written as either a product of Xs or product of Zs, these are called as CSS code. From this definition, one can see that majority of the proposed models for quantum memories fall into this category.[1, 2, 12–16] When studying the stability of these models, one can show that one of the codes can protect classical information from thermal fluctuation while the other one cannot. This means that there is a manifest difference between how the models treat the bit flip error and the phase flip error. Chamon's model treats X, Y, and Z error in an identical manner but it lacks stability in thermal sense.[17, 18] Since we expect a singular behavior at the phase boundary between an 'ordered state' and 'disordered state' for thermally stable quantum memory, absence of finite-temperature phase transition seems troublesome unless there is an argument that can evade this logic. Motivated by these ideas, we present a new spin-$\frac{1}{2}$ model with finite temperature phase transition whose ground state is a non-CSS quantum error correcting code. Our model exhibits a topological order, but only the classical part survives in finite temperature.

The outline of the paper is as follows. We set the stage by introducing the hamiltonian in Section II. In Section III, we study the quantum code that defines the ground state of the hamiltonian. We calculate the number of qubits and find the logical operators. In Section IV, we study the low-energy excitation of the hamiltonian that consists of particles and closed strings. We construct a duality relation with classical Ising model in Section V to show the finite temperature phase transition.

II. MODEL

We place qubits on a vertices of a 4-valent 3D lattice. Using the notation $X_i \equiv \sigma_i^x$, $Y_i \equiv \sigma_i^y$, $Z_i \equiv \sigma_i^z$ stabilizer generators are

$$B_p^x = \Pi_{i\in p} X_i \tag{2.1}$$

$$B_p^y = \Pi_{i\in p} Y_i \tag{2.2}$$

$$B_p^z = \Pi_{i\in p} Z_i, \tag{2.3}$$

where p is the plaquette and $\{i \in p\}$ denotes a set of vertices on plaquette p. We shall partition a set of plaquettes into P_x, P_y, P_z, which corresponds to a set of nontrivial supports for B_p^x, B_p^y, B_p^z. We shall call elements of these sets as $X-, Y-, Z-$plaquettes.

Our model is inspired by the construction of topological color code in 3D.[14] For this quantum code, qubits reside on the vertices of the lattice, and the lattice is locally 4-valent. The stabilizer generators are either a product of Xs or product of Zs, and they correspond to the unit cells of different dimensions; in one example, generators are either in cubic form or plaquette form. Our approach differs in a sense that we only allow plaquette operators as stabilizer generators.

Local description of our model can be seen in FIG.1(a). At each vertex, there are 6 plaquette operators that have nontrivial support on it. Each plaquette operators meet with a same kind of plaquette operator on each vertices and meet with 4 other plaquette operators on 2 vertices. Thus the assignment in FIG.1(a) guarantees commutativity between the stabilizer

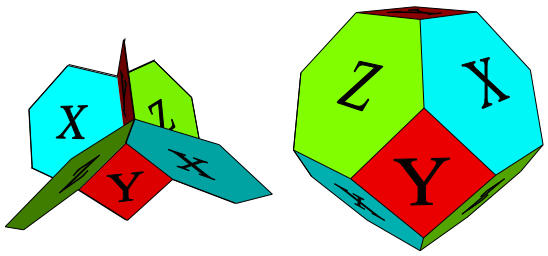

(a) Vertex Figure (b) Unit Cell

FIG. 1: (Color online)Vertex figure and unit cell of our model. Qubits reside on the vertices. One can see that $B^x_{p_x}$ meets with another $B^x_{p_x}$ at one vertex whereas it meets with $B^y_{p_y}$ and $B^z_{p_z}$ at two vertices.

operators. We must point out that not every lattice structure allows vertex figure like FIG.1(a). There are only 4 translationally invariant convex tessellations that have tetrahedral vertex figure: bitruncated qubic honeycomb, cantitruncated cubic honeycomb, omnitruncated cubic honeycomb, and cantitruncated alternated cubic honeycomb.[22] Only the first three admits an arrangement of plaquette operators similar to FIG.1(a) at every vertex. In this paper, we mainly study the bitruncated qubic honeycomb model for its simplicity but analogous results shall be discussed in full generality if possible. Unit cell is shown in FIG.1(b) and tessellation is shown in FIG.2. Bitruncated qubic honeycomb is a space-filling tessellation made up of truncated octahedra. It has 14 faces, 36 edges, and 24 vertices. There are 6 square faces and 8 hexagonal faces. Without loss of generality, one can set the 6 square faces to be Y plaquette operator, 4 of the hexagonal faces to be X plaquette operator and 4 remaining hexagonal faces to be Z plaquette operators.Hamiltonian is a sum over the plaquette operators.

$$H = -J\Big(\sum_{p_x\in P_x} B^x_{p_x} + \sum_{p_y\in P_y} B^y_{p_y} + \sum_{p_z\in P_z} B^z_{p_z}\Big). \tag{2.4}$$

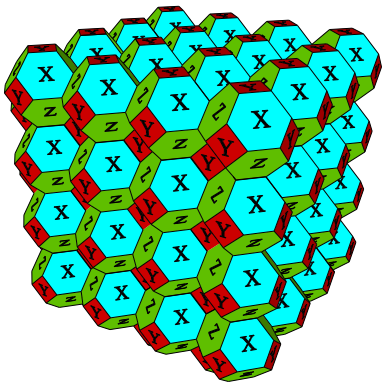

FIG. 2: (Color online)Arrangement of stabilizer generators. Translation of unit cells form a tessellation.

III. QUANTUM CODE

Purpose of this section is to study the quantum code generated by a set of group generators $\{B^x_{p_x}, B^y_{p_y}, B^z_{p_z}\}$. We start with introducing the notation and definition that shall be used throughout the analysis. Rest of the section is mainly divided into two parts. In Section III B, we count the number of encoded qubits. In Section III C, we completely specify a set of logical operators for each qubits.

A. Preliminary Results

Given a CW-complex, Euler characteristic χ can be defined as an alternating sum of k_ns, where k_n denotes a number of cells of dimension n.

$$\chi = \sum_{i=0}^{d} k_i(-1)^i \tag{3.1}$$

For instance, if we consider a 2-dimensional manifold, k_0 is a number of vertices, k_1 a number of edges, and k_2 a number of faces. One of the main idea that we used in this paper is that χ can be also written as an alternating sum of betti number b_is.

$$\chi = \sum_{i=0}^{d} b_i(-1)^i \tag{3.2}$$

b_i is the rank of the n-th singular homotopy group, but for odd-dimensional closed orientable manifold it is not necessary to calculate each individual b_is. This is due to Poincaré duality: although it has various different forms, for the purpose of our paper, we can use the one originally introduced by Poincaré himself.

Theorem 1 *(Poincaré, 1895)* $b_k = b_{d-k}$ *for a closed orientable d-dimensional manifold.*

From this theorem, one can easily deduce that $\chi = 0$ for odd dimensional closed orientable manifold.

B. Number of Encoded Qubits

Number of encoded qubits can be computed from the size of the stabilizer group and the number of physical qubits. Since the plaquette operators are not independent to each other, we must count the number of independent relations. In such pursuit, geometrical interpretation of our model becomes useful. We would first like to point out that multiplying all the plaquette operators on a unit cell reduces to identity. One can see this from FIG.1(b). Since any contractible closed surface on the lattice can be represented as a union of unit cells, one can see that multiplication of plaquette operators on *any* contractible closed surface reduces to identity. Therefore we have $C-1$ independent relations which generate smooth deformation, where C is the number of unit cells. We must subtract 1 because multiplying all but one cell results in a relation for that very cell.

Let us consider a periodic boundary condition on all 3 directions. There exists noncontractible surface that reduces to identity as one can see in FIG.3(a), FIG.3(b). Since there are 3 topologically distinct noncontractible surfaces, we have 3 independent relations, resulting in $C+2$ independent relations. Finally, multiplying all X-like operators adds one independent relation. One can check that multiplication of Ys and multiplication of Zs are implied by the previously mentioned relations.

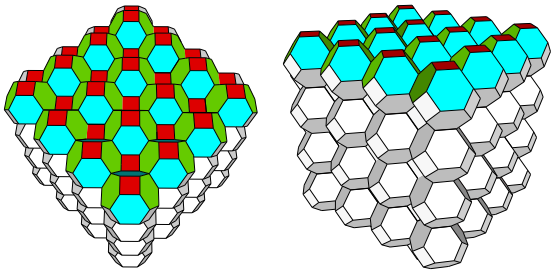

(a) Top View (b) Side View

FIG. 3: (Color online)Representation of nontrivial constraints between the stabilizer operators. One can see that multiplication of all the plaquette operators on a noncontractible closed surface reduces to identity. At each vertex, there are either 1) exactly one X, one Y, and one Z or 2) two Xs and two Zs.

Accounting for these relations, number of encoded qubits is $V-F+C+3=3$, where V is the number of vertices, F is the number of faces, and C is the number of unit cells. First two correspond to the number of qubits and number of plaquette operators. The remaining terms represent a number of independent relations between plaquette operators. We shall show that in fact the number of encoded qubits only depend on the second Betti number, b_2.

Lemma 1 *For stabilizer group* $\{B^x_{p_x}, B^y_{p_y}, B^z_{p_z}\}$, *number of encoded qubits is* b_2.

Proof : Let us consider the dual lattice. This can be constructed by replacing k-dimensional object into a $(d-k)$-dimensional object. For instance, vertices of the dual lattice resides on the center of the unit cells of the original lattice. Faces on the dual lattice can be constructed by connecting the edges so that the resulting surface is perpendicular to the edges in the original lattice. Euler characteristic χ is trivially 0 due to Poincaré Duality. The unit cells of the resulting dual lattice is an irregular tetrahedron. Let us denote k_is to be number of i-dimensional cells on the *dual lattice*. One can see that V, the total number of vertices in the original lattice becomes k_3, a number of unit cells in the dual lattice. Similarly, F is identical to k_1 and C is identical to k_0. Note that $k_2 = k_3$, for each cell contains 4 faces and each faces meet with two tetrahedral cells. Therefore, we have

$$V-(F-C) = k_3 - k_1 + k_0 \tag{3.3}$$
$$= -k_3 + k_2 - k_1 + k_0 = 0 \tag{3.4}$$

Hence

$$k = V-(F-(C-1+1+b_2)) \tag{3.5}$$
$$= b_2, \tag{3.6}$$

where b_2 is the second Betti number of the manifold. One can also use this intuition to prove that the group generated by the plaquette operators does not contain $-I$.

Lemma 2 $\langle B^x_{p_x}, B^y_{p_y}, B^z_{p_z}\rangle$ *does not contain* $-I$.

Proof: Consider a product of plaquette operators that is proportional to the identity operator. Any such configuration can be generated by product of all X-plaquette operators, product of all Y-plaquette operators, product of all Z-plaquette operators, product of plaquettes along a closed surface. The first three are trivially $+I$. For unit cells, we have 24 vertices at which X,Y, and Z meets. Since all the generators commute with each other, we can arrange the product to be in the following canonical form.

$$\Pi_{p_x} B^x_{p_x} \Pi_{p_y} B^y_{p_y} \Pi_{p_z} B^z_{p_z}. \tag{3.7}$$

Since $XYZ = i$, the product of plaquette operators on a unit cell is 1. Similarly, product of plaquette operators on a noncontractible surface described in FIG.3(a), FIG.3(b), we have $4n$ vertices where X,Y, and Z meets. Hence we arrive at the same conclusion. Since any product of plaquette operators that results in a trivial operator can be constructed by these constraints, the group does not contain $-I$.

C. Logical Operators

There are two logical operators that are reminiscent to the surface and string operator of 3D toric code. These are drawn in FIG.4. One can see the surface operator on the top of the lattice system which is a product of $B^z_{p_y}$s on one layer of Y-plaquettes. The complementary logical operator to this is the string operator that has a sequence of $YZYXYZYXYZYX\cdots$ along the line perpendicular to the surface operator. This string winds around the torus and completes a noncontractible loop. These two operators anticommute with each other and both of them commute with the stabilizer generators. We can similarly define two sets of complementary operators in other directions. One can easily check the expected commutation and anticommutation relations.

IV. LOW ENERGY EXCITATION

Quasiparticles excitations in 2D typically arise as anyons. For instance, in Kitaev's toric code, two quasiparticles are created in pair, and when fused together, they vanish.[1] There are two kind of particles analogous to electric and magnetic charge, and when one particle winds around another one, the system attains a nontrivial global phase. In 3D, trajectory of winding around another particle can be deformed into a trivial contour. Hence one needs higher dimensional object to attain

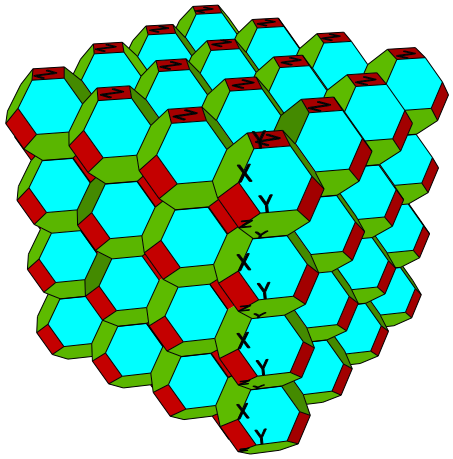

FIG. 4: (Color online)There is one surface operator and one string operator for each qubits. Surface operator corresponds to the product of $ZZZZ$ on Y-plaquettes. String operator is the line perpendicular to this surface, showing a sequence $YZYXYZYX\cdots$.

a similar topological action. In 3D there are closed string-like excitations and particle-like excitations.[2, 13] When the particle winds around the string so that the trajectory and the string together forms a knot, the system attains a nontrivial global phase.

Our model presents a similar picture. Particle-like excitations are created in pair. If we truncate a string-like logical operator, excitations form at the end points. When the particle-antiparticle pair is created, they can diffuse without any extra energy cost. Closed string-like excitations can be similarly thought as a truncated surface-like logical operator. Near the boundary of the surface, there are excitations and hence the energy cost grows linearly with the size of the surface. When a particle penetrates the closed string, we find that

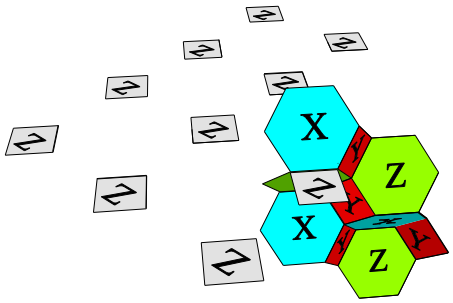

FIG. 5: (Color online)Representation of particle penetrating through a string-like excitation. Truncated surface operator is a product of Z-plaquettes in white. Trajectory of the particle is a nontrivial support of the colored plaquette operators, which coincides with the Z-surface.

$$|\psi_{Initial}\rangle = SP|\Phi\rangle \tag{4.1}$$
$$|\psi_{Final}\rangle = USP|\Phi\rangle = -|\psi_{Initial}\rangle, \tag{4.2}$$

where S is a closed-string excitation, P is a particle excitation, and U is a trajectory of the particle. Thus system gains $e^{i\pi}$ phase factor. This is illustrated in FIG.5. One can see that as a particle penetrates through the surface operator and returns to the original position, it coincides with the surface operator at one vertex, thus giving the anticommutation relation.

Low energy excitation in terms of elementary objects provides us an intuitive picture for the thermal stability. Particles can be created out of vacuum in pair and propagate freely. They can diffuse and wind around the torus to induce logical error. Closed strings, on the other hand, need energy that is proportional to its perimeter. Given a closed string-like excitation as in FIG.5, the stabilizer generators anticommuting with the surface operator only reside near the boundary of the surface. Z-plaquettes trivially commute with the surface operator. X-plaquettes commute with the surface operator since they meet at two vertices. However, there are Y-plaquettes meeting at exactly one vertex at the boundary. Hence we expect our system to be a stable classical memory.

V. DUALITY

Typical strong-weak duality relation relates a strong coupling limit of one model to a weak coupling limit of another model: we use a slightly different strategy here. We first show that our model can be mapped into an Ising gauge theory, from which we can use the Wegner-type duality relation with Ising model. Mapping from our model to Ising gauge theory is not exact for finite sized lattice, but this difference vanishes in the thermodynamic limit. Starting from the partition function of our model,

$$Z = tr(\exp(-\beta H)) \tag{5.1}$$
$$= tr(\Pi_{S_i\in S}(\cosh\beta J + S_i \sinh\beta J)), \tag{5.2}$$

where $S_i \in \{B^x_{p_x}, B^y_{p_y}, B^z_{p_z}\}$,

$$Z = (\cosh\beta J)^n tr(\Pi_i(1+\alpha S_i)) \tag{5.3}$$
$$= (\cosh\beta J)^n tr(\sum_{\{k_i\}=0}^{1} \Pi_i \alpha^{k_i} S_i^{k_i}). \tag{5.4}$$

Since the Pauli operators are traceless, the nonvanishing terms correspond to the nontrivial constraints presented in Section III B. Note that there were two kind of constraints: constraints coming from the closed 2-manifold and constraints coming from space-filling products of X, Ys, or Zs. Using this, we can write down the partition function in the following form.

$$Z = (2\cosh\beta J)^n(\sum_c \alpha^{A_c} + (1+\alpha^{n_x})(1+\alpha^{n_y})(1+\alpha^{n_z}) - 1 + C.T.) \tag{5.5}$$

$\sum_c$ is a sum over a configuration of closed 2-manifolds. A_c is the number of plaquettes for each configurations. $C.T.$ corresponds to the cross terms between closed 2-manifolds and space-filling product of Xs, Ys, or Zs. $n_{x,y,z}$ corresponds to the number of $X,Y,Z-$plaquette operators. The main idea is that the partition function is dominated by the first term in the thermodynamic limit. We show this in Appendix A.

Lemma 3 *$Z - C.T. - (\alpha^{n_x} + \alpha^{n_y} + \alpha^{n_z}) = Z_{IG}(\beta J)$, where Z_{IG} is a partition function of Ising gauge theory on the same lattice with temperature β and coupling constant J.*

Proof : Consider a mapping $B^x_{p_x} \to ZZZZZZ$, $B^y_{p_y} \to ZZZZ$, $B^z_{p_z} \to ZZZZZZ$, where $Z\cdots Z$ are products of Z on the edges of each plaquettes. The resulting model is an Ising gauge theory on a bitrucated cubic honeycomb. Partition function is

$$Z_{IG} = tr(\exp(-\beta H)) \tag{5.6}$$
$$= (\cosh\beta J)^n tr(1 + \tanh\beta J S_i), \tag{5.7}$$

where S_is are either $ZZZZZZ$ or $ZZZZ$ depending on the plaquette. Since Pauli operators are traceless, only a product of plaquette operators that are union of closed surface survives. Therefore, we conclude

$$Z_{IG}(\beta J) = Z - C.T. - (\alpha^{n_x} + \alpha^{n_y} + \alpha^{n_z}). \tag{5.8}$$

Using the duality relation between Ising gauge theory and Ising model, we can map our model into an Ising model. We show the duality relation in Appendix B.

Theorem 2 *Our model with coupling constant βJ is dual to the classical Ising model on a dual lattice with a dual coupling constant $\tilde{\beta}\tilde{J} = -\frac{1}{2}\ln\tanh\beta J$.*

Since the Ising model undergoes a finite temperature phase transition, so does our model. This is analogous to the behavior of 3D toric code under temperature change. As in our model, one can show that 3D toric code has critical temperature by using the duality relation with Ising model. Below the critical temperature, there is a symmetry breaking with respect to a surface-like logical operator. Symmetry associated to the string-like logical operator is broken only at the ground state.

One glaring difference though, is that 3D toric code can be decomposed into two classical hamiltonians without spoiling the phase transition: the hamiltonian responsible for correcting the bit flip error is identical to Ising gauge theory, which has finite temperature phase transition. On the other hand, the hamiltonian responsible for correcting the phase flip error does not have a phase transition. Hence one can intuitively understand that 3D toric code can only correct bit flip errors but not phase flip errors under thermal equilibrium. Our model does not allow such decomposition. Once we get rid of any of $B^x_{p_x}, B^y_{p_y}$, or $B^z_{p_z}$, the partition function does not exhibit a phase transition any more. This shows that non-CSS code with finite temperature phase transition in 3D does not necessarily provide a self-correcting quantum memory.

VI. CONCLUSION

In this paper, we studied an exactly solvable 3D spin model and studied its topological order. The ground state of the system defines a non-CSS quantum error correcting code. At finite temperature, this system is expected to behave as a stable classical memory, but not as a stable quantum memory. This is mainly due to the fact that there exists a string-like logical operator. In light of studying the possibility of self-correcting quantum memory, this reconfirms the general properties that have been found in 3D stabilizer codes so far: for each encoded qubit, there exists one surface-like logical operator and one string-like logical operator. It seems that we cannot avoid such outcome unless the shape of the logical operator changes as the system size changes, as in Chamon's model.[17, 18] This in fact was recently argued to be the general feature of stabilizer codes whose number of encoded qubits remain invariant under system size change. [23]

It is worth noting that the thermal stability analysis of our model is not rigorous at this stage, even though the energy barrier increasing as the perimeter of the surface is a compelling evidence that this must be true. It would be desirable to make a rigorous estimate of thermal relaxation rate using the method introduced by Chesi et al.[24] We expect the string-like logical operator to be thermally fragile and the surface-like logical operator to be stable. As in 3D toric code,[13] we also expect the topological entropy of our model to show a singular behavior near the critical point. These singular behavior arise due to the existence of finite temperature phase transition, which we can show rigorously by the strong-weak duality relation between our quantum model to a classical Ising model on the dual lattice.

Acknowledgments

Author would like to thank Jeongwan Haah for his help in finding the logical operator of the system, and John Preskill for many insightful discussions. This research was supported in part by NSF under Grant No. PHY-0803371 and ARO under Grant No. W911NF-09-1-0442.

Appendix A: Bound for the cross terms.

Corss term can be written as

$$C.T. = \sum_c \alpha^{A_c} \sum_{i\in\{x,y,z\}} \alpha^{n_i - 2n_i^c}, \tag{A1}$$

where n_x, n_y, n_z are total number of $X,Y,Z-$plaquettes and n_x^c, n_y^c, n_z^c are number of $X,Y,Z-$plaquettes for configuration c.

Lemma 4 *There exists* $0 < \varepsilon_{1,2} < 1$ *such that*

$$A_c + n_i - 2n_i^c \geq \varepsilon_1 A_c + \varepsilon_2 n_i \tag{A2}$$

for $\forall c, i$.

Proof : Consider $i = x$. Left hand side of the inequality is

$$n_y^c + n_z^c - n_x^c + n_x \geq n_y^c + n_z^c - (1-\varepsilon)n_x^c + (1-\varepsilon)n_x \tag{A3}$$

$$\geq (\frac{\varepsilon}{2})A_c + (1-\varepsilon)n_x \tag{A4}$$

On the second line, we used the fact that the minimum is achieved in the case where $n_y^c = 0$, implying $n_z^c = n_x^c = \frac{1}{2}A_c$. Same logic can be applied to $i = z$. For $i = y$,

$$n_x^c + n_z^c - n_x^c + n_y \geq n_x^c + n_z^c - (1-\varepsilon)n_y^c + (1-\varepsilon)n_y \tag{A5}$$

$$\geq (\frac{2}{5} - \frac{3}{5}(1-\varepsilon))A_c + (1-\varepsilon)n_y. \tag{A6}$$

Similarly, here we used the fact that the minimum is achieved in the case where one of n_x^c or n_z^c is 0. Then we have a $2:3$ ratio between the $X-(Z-)$plaquettes and $Y-$plaquettes. Therefore, for $\varepsilon > \frac{1}{3}$, we have such $(\varepsilon_1, \varepsilon_2)$.

Lemma 5

$$\lim_{vol\to\infty} \frac{Z(\beta J)}{Z_{IG}(\beta J)} \to 1. \tag{A7}$$

, where $Z_{IG}(\beta J)$ *is a partition function for Ising gauge theory with temperature* β *and coupling constant* J*. vol is the volume of the lattice.*

Proof :

We use

$$\sum_c \alpha^{\varepsilon_1 A_c} = \frac{(2\cosh\beta J')^n}{(2\cosh\beta J')^n} \sum_c \alpha^{\prime A_c} \tag{A8}$$

$$= (\frac{1}{2\cosh\beta J'})^n Z_{IG}(\beta J'), \tag{A9}$$

where

$$\tanh\beta J' = (\tanh\beta J)^{\varepsilon_1}. \tag{A10}$$

Thus the cross terms can be bound by

$$Z_{IG}(\beta J')(\frac{\cosh\beta J}{\cosh\beta J'})^n \alpha^{\delta_i \varepsilon_2 n}, . \tag{A11}$$

where $\delta_i = \frac{n_i}{n}$,where n is the total number of plaquettes. This becomes

$$Z_{IG}(\beta J')((\frac{1-t^2}{1-t^{\frac{2}{\varepsilon_1}}})^{\frac{1}{2}} t^{\frac{\varepsilon_2}{\delta\varepsilon_1}})^n, \tag{A12}$$

where $t = \tanh\beta J'$. One can show that $(\frac{1-t^2}{1-t^{\frac{2}{\varepsilon_1}}})^{\frac{1}{2}} t^{\frac{\varepsilon_2}{\varepsilon_1\delta}} < 1$ for $\beta J > 0$. Since the renormalized coupling constant J' is larger than J, we can see that these correction terms become negligible in thermodyamic limit. Therefore,

$$|\lim_{vol\to\infty} \frac{Z(\beta J) - Z_{IG}(\beta J)}{Z_{IG}(\beta J)}| \leq |\frac{Z_{IG}(\beta J')}{Z_{IG}(\beta J)}\lambda^n + O(\alpha^n)|, \tag{A13}$$

where $J' > J$ and $0 < \lambda < 1$. In $n \to \infty$ limit, we get the desired result.

Appendix B: Duality between Ising gauge theory and Ising model

Lemma 6 *Ising gauge theory on bitruncated cubic honeycomb is dual to Ising model on the dual lattice.*

Proof:

$$Z = (\cosh\beta J)^n tr(\Pi_i(1 + \tanh\beta J S_i)) \tag{B1}$$

$$= (\cosh\beta J)^n tr(\sum_{\{k_i\}=0}^{1} \Pi_i \alpha^{k_i} S_i^{k_i}) \tag{B2}$$

$$= (2\cosh\beta J)^n \sum_{\{k_i\}=0}^{1} \Pi_i \alpha^{k_i} \Pi_e \delta_2(\sum_j k_{j;e}), \tag{B3}$$

where Π_e is a product over all the edges and $\sum_j k_{j;e}$ is a sum over k_js that have nontrivial support on edge e. There are three such k_js. One can use $k_{j;e} = \frac{1}{2}(1 - ZZ)$, where ZZ is a product of Zs on qubits that reside on the vertices of the dual lattice. For 8 spin configurations $(Z_1, Z_2, Z_3) = (-1,-1,-1), (1,1,1), (1,-1,-1), (-1,1,-1), (-1,-1,1), (1,1,-1), (-1,1,1), (1,-1,1)$, one can see that all of these configurations satisfy the delta function. Furthermore, we have 2 combinations for $(k_1, k_2, k_3) = (0,0,0)$, 2 combinations for $(0,1,1)$, $(1,0,1)$, and $(1,1,0)$. Plugging this in, we get

$$Z = (\cosh\beta J)^n \sum_{\{Z_i\}=0}^{1} \Pi_i \alpha^{1 - \frac{1}{2} Z_{i+\hat{n}_i} Z_{i-\hat{n}_i}}, \tag{B4}$$

where $Z_{i\pm\hat{n}_i}$ is the Z operator on the dual sites of plaquette i. $\hat{n}_i$ is the unit normal vector to the plaquette. Therefore, up to a constant, partition function is identical to the partition of Ising model with $\tilde{\beta J} = -\frac{1}{2}\ln\tanh\beta J$.

[1] A. Y. Kitaev, Annals Phys. **303**, 2 (2003).
[2] H. Bombin and M. A. Martin-Delgado, Phys.Rev.Lett. **97**, 180501 (2006).
[3] A. Kitaev, Annals of Physics **321**, 2 (2006).
[4] P. Fendley and E. Fradkin, Phys.Rev. B **72**, 024412 (2005).
[5] A. Ioselevich, D. A. Ivanov, and M. V. Feigelman, Phys. Rev. B **66,**, 174405 (2002).
[6] M. A. Levin and X.-G. Wen, Phys.Rev. B **71**, 045110 (2005).
[7] R. Moessner and S. L. Sondhi, Phys. Rev. Lett **86,**, 1881 (2001).
[8] S. Bravyi, D. Poulin, and B. Terhal, Phys. Rev. Lett. **104**, 050503 (2010).
[9] S. Bravyi and B. Terhal, New J. Phys. **11**, 043029 (2008).
[10] E. Dennis, A. Kitaev, A. Landahl, and J. Preskill, J. Math. Phys. **43,**, 4452 (2002).
[11] R. Alicki, M. Horodecki, P. Horodecki, and R. Horodecki, Open Syst. Inf. Dyn. **17**, 1 (2008).
[12] M. H. H. Bombin, R. W. Chhajlany and M. Martin-Delgado, arXiv:0907.5228 (2009).
[13] C. Castelnovo and C. Chamon, Phys. Rev. B **78**, 155120 (2008).
[14] H. Bombin and M. A. Martin-Delgado, Phys.Rev.B **75**, 075103 (2007).
[15] Z. Nussinov and G. Ortiz, Phys. Rev. B **77**, 064302 (2008).
[16] Z. Nussinov and G. Ortiz, Ann. Phys. **324**, 977 (2009).
[17] C. Chamon, Phys. Rev. Lett. **94,**, 040402 (2005).
[18] S. Bravyi, B. Leemhuis, and B. M. Terhal (2010).
[19] A. R. Calderbank and P. W. Shor, Phys. Rev. A **54**, 1098 (1996).
[20] A. M. Steane, Phys. Rev. A **54**, 4741 (1996).
[21] D. Gottesman, Ph.D Thesis, Caltech (1997).
[22] B. Grünbaum, Geombinatorics **4**, 49 (1994).
[23] B. Yoshida, arXiv:1007.4601 (2010).
[24] S. Chesi, D. Loss, S. Bravyi, and B. M. Terhal, New J. Phys. **12,**, 025013 (2009).